15th Triennial World Congress, Barcelona, Spain

INPUT SHAPING CONTROL OF CONTAINER CRANE SYSTEMS: LIMITING THE TRANSIENT SWAY ANGLE

Chang-Do Huh[a] and Keum-Shik Hong[b]

[a] *Department of Mechanical and Intelligent Systems Engineering, Pusan National University, 30 Jangjeon-Dong, Kumjeong-Ku, Pusan, 609-735, Korea.*
Tel: +82-51-510-1481, Fax: +82-51-514-0685, Email: cdhuh@pusan.ac.kr
[b] *School of Mechanical Engineering, Pusan National University, 30 Jangjeon-Dong Kumjeong-Ku, Pusan 609-735, Korea. Tel: +82-51-510-2454, Fax: +82-51-514-0685*
Email: kshong@pusan.ac.kr

Abstract: A modified input shaping control to reduce residual vibration at the end-point and to limit the sway angle of the payload during traveling for container crane systems is investigated. When the maneuvering time is minimized, a large transient amplitude and steady state oscillations may occur inherently. Since a large swing of the payload during the transfer is dangerous, the control objective is to transfer a payload to the desired place as quickly as possible while limiting the swing angle of the payload during the transfer. The conventional shapers are enhanced by adding one more constraint to limit the intermediate sway angle of the payload. The developed method is shown to be more effective than other conventional shapers for preventing an excessive transient sway. Computer simulation results are provided. *Copyright © 2002 IFAC*

Keywords: crane system, input shaping control, feedforward control, time-optimal control, residual vibration, robustness

1. INTRODUCTION

The efficiency of cargo handling work at a port or at an industry field depends largely on the operation of cranes. For example, when a ship is unloaded, containers are first transferred from the ship to a waiting truck by a container crane as shown in Fig. 1. The truck then carries the container to an open storage area, where another crane stacks the container to a pre-assigned place. The bottleneck of this cycle lies in the transfer of the containers from the ship to the truck. Therefore, minimizing this transfer time will bring about a large cost saving. Since a large swing of the container load during the transfer is dangerous, the problem is to transfer a container to the desired place as quickly as possible while minimizing the swing of the container during transfer as well as the swing at the end of transfer.

When the swing is considered, a time-optimal flexible-body command that results in zero residual vibration can be generated (Auernig and Troger, 1987). Hoisting of the load during the transverse motion of the trolley increases the difficulty of generating the control input because the system is nonlinear time-varying. If the system model is linearized, then the associated frequency is time-varying. Optimal controls based on a nonlinear model are difficult in general (Moustafa and Ebeid, 1988). One method for developing optimal controls divides the crane motion into five different sections (Sakawa and Shindo, 1982). However, even when optimal inputs can be generated, implementation is usually impractical because the boundary conditions at the end of the maneuver (move distance) must be known at the start of the move. Six different velocity patterns of trolley movement including trapezoidal, stepped, and notched patterns were compared in Hong et al. (1997). A two-stage control strategy which combines a time-optimal traveling and a nonlinear residual sway control was presented in Hong et al. (2000).

The very interesting technique by Smith (1958) proposes the split of input excitation into several segments in the fashion that the sum of all transient terms is equal to zero after the last excitation. This technique was referred to as the posicast technique. This work, however, lacks the robustness to errors in estimated damping and frequency of the controlled system. Recently, the posicast technique, named as input shaping, has been re-illuminated by a group of people at MIT and rigorous theory has been

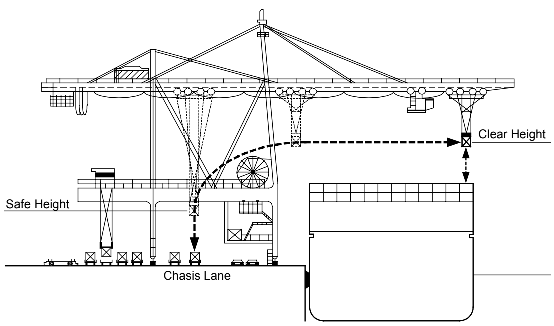

Fig. 1 A container crane system.

established (Singer and Seering, 1990; Singhose et al., 1994).

Considerable works have been done in recent years on the topics of positioning and slewing using the input shaping method. Time-optimal rest-to-rest slewing of flexible systems has been investigated by several researchers (Liu and Wie, 1992). Examples of input shaping applications include a Cartesian robot (Meckl and Seering, 1990), industrial robots (Park and Chang, 1998), and crane systems (Park et al., 2000; Singhose et al., 2000). Flexible systems equipped with constant force actuators can use input shaping technique by switching the actuators on and off at appropriate times (Singhose et al., 1997).

This paper presents a modified input shaping control methodology to restrict the swing angle of the payload within a specified value during the transfer as well as to minimize the residual vibration at the end-point. The conventional design method is enhanced by adding one more constraint to limit the transient sway angle within a specified value using the sway angle equation based on a linear time-invariant system. A similar approach, limiting the magnitude of transient motion, has been investigated by Singhose et al. (1997), but in their work the command profiles were based upon on/off constant force actuators and a limitation was set on the maximum acceleration, not on the maximum velocity. In real situations, the system saturations occur not only during acceleration but also in achieving the maximum velocity. In this paper the command profiles are generated by convolving a time-optimal rigid-body command signal that satisfies given constraints and an appropriate shaper. Simulation results of the conventional shapers and the proposed ones are compared in terms of the amplitude of the transient sway angle, residual sway distance, robustness in natural frequency discrepancy, and traveling time. The proposed method is easier to implement compared with the conventional time-optimal control and robust control schemes and does not require any feedback signal. Rather than attempting to obtain exactly zero residual vibration, which is practically impossible, this technique yields non-zero but low levels of vibration.

2. CONTROL PROBLEM FORMULATION

2.1 Crane System: Modeling

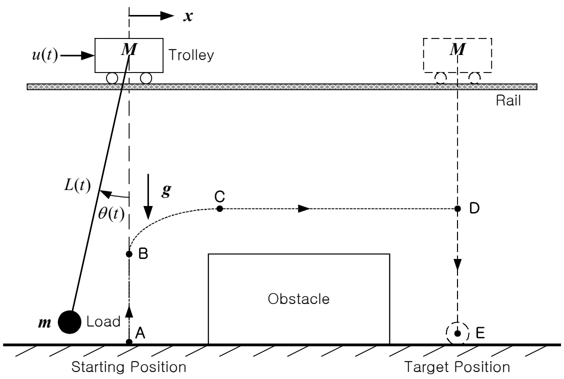

Fig. 2 A schematic diagram for the payload movement.

Table 1 Specifications of the crane and simulation parameters.

	Traveling	Hoisting
Maximum acceleration	0.2 m/s^2	0.1 m/s^2
Maximum velocity	1.0 m/s	0.5 m/s
< Simulation Parameters > - The traveling distance from B to D: 30 m - The rope length at B: 21 m - The rope length at C: 15 m		

Three different equations of motion about the crane system depicted in Fig. 2 can be derived.

(1) *Nonlinear System*

$$L(t)\ddot{\theta}(t)+2\dot{L}(t)\dot{\theta}(t)+g\sin\theta(t)=\cos\theta(t)u(t)\,, \quad (1)$$

where $L(t)$ is the time-varying rope length in meter, $\theta(t)$ is the sway angle in radian, g is the gravitational acceleration, and $u(t)$ is the acceleration of the trolley, which is the control input.

(2) *Linear Time-Varying System*

If the sway angle $\theta(t)$ is small enough, $\sin\theta(t)\approx\theta(t)$ and $\cos\theta(t)\approx 1$, then (1) can be linearized as follows:

$$L(t)\ddot{\theta}(t)+2\dot{L}(t)\dot{\theta}(t)+g\theta(t)=u(t)\,. \quad (2)$$

(3) *Linear Time-Invariant System*

In this model, the hoisting is not considered. That is, the rope length is fixed at a constant value. And then, the simplest model of a container crane is derived as follows:

$$L\ddot{\theta}(t)+g\theta(t)=u(t)\,. \quad (3)$$

2.2 Path Planning

The cycle is divided into four paths as shown in Fig. 2. The four paths are described separately for the purpose of facilitating understanding of the semi-automatic modes. In this paper, path BD is the control range.

(1) *Path AB*: Hoisting up (manual mode)
(2) *Path BC*: Hoisting up and traveling of the trolley (auto mode)
(3) *Path CD*: Traveling of the trolley (auto mode)
(4) *Path DE*: Hoisting down (manual mode)

2.3 Specifications of the Crane

Specifications of the crane and simulation parameters are summarized in Table 1. Here, the simulation parameters may be different from the real operation values in the industry.

2.4 Control Performance Specifications

In this paper, the control performance specifications are to maintain sway angle during traveling within 0.0120 radian (about 0.7°) and to bring the payload to a stop within $\pm$ 30 mm at terminal rope length.

3. CONVENTIONAL INPUT SHAPING CONTROL

Input shaping is a feedforward control technique for improving the settling time and the positioning accuracy, while minimizing residual vibrations, of servo systems with the flexible mode. The method works by creating a input signal that cancels its own vibration. That is, vibration caused by the first part of the input signal is canceled by vibration caused by the second part of the input.

3.1 Basic Constraints for Solving Input Shaper

The angle constraint in Section 4, which is the main part of this paper, is one additional constraint on top of the basic constraints. Hence, to complete all necessary constraints and to help readers to understand, the fundamental concept of the input shaping method is briefly summarized from the work of (Singer and Seering, 1990) in this subsection. The constraints are based on the assumption that the system can be treated as a superposition of linear time-invariant (LTI) second-order systems.

The constraint on vibration amplitude can be expressed as the ratio of residual vibration amplitude with shaping to that without shaping. This vibration percentage can be determined by using the expression for residual vibration of a second-order harmonic oscillator of frequency ω rad/sec and damping ratio ζ . The vibration from a series of impulses is divided by that from a single impulse to get the vibration percentage as follows:

$$V(\omega,\zeta) = e^{-\zeta\omega t_N}\sqrt{(C(\omega,\zeta))^2+(S(\omega,\zeta))^2}\ , \qquad (4)$$

where

$$C(\omega,\zeta) = \sum_{i=1}^{N} A_i e^{\zeta\omega t_i}\cos(\omega\sqrt{1-\zeta^2}\,t_i)\ ,$$

$$S(\omega,\zeta) = \sum_{i=1}^{N} A_i e^{\zeta\omega t_i}\sin(\omega\sqrt{1-\zeta^2}\,t_i)\ .$$

N is the number of impulses in the input shaper, A_i and t_i are the amplitudes and time locations of the impulses, t_N is the time of the last impulse, and ω and ζ are the natural frequency and damping ratio of the flexible mode of the system.

Additional constraints require that the impulses always sum to one and the shaper be as short as possible. These constraints ensure that the desired setpoint will be achieved with a minimum time delay.

$$\sum_{i=1}^{N} A_i = 1\ , \qquad (5)$$

$$\min(t_N)\ . \qquad (6)$$

If the constraint equations require only zero residual vibration $(V=0)$, then the resulting shaper is called a zero vibration (ZV) shaper. The earliest appearance of ZV shaping was the technique of posicast control developed in the 1950's (Smith, 1958).

For input shaping to work well on most real systems, the constraint equations must ensure robustness to modeling errors. The earliest form of robust input shaping to errors in the system parameters was achieved by setting the partial derivative with respect to the frequency of the residual vibration equal to zero, that is:

$$0 = \frac{\partial}{\partial\omega}V(\omega,\zeta). \qquad (7)$$

The resulting shaper is called a zero vibration and derivative (ZVD) shaper. The ZVD shaper is much more robust to modeling errors than the ZV shaper. However, the ZVD shaper has a time duration equal to one period of the vibration, as opposed to the one-half period length of the ZV shaper.

An alternate procedure for increasing insensitivity uses extra-insensitivity (EI) constraints (Singhose et al., 1994). Instead of restricting the residual vibration to zero at the modeling frequency, the residual vibration is limited to a low level, so-called a tolerable vibration, V_{tol} . The EI shaper achieves an increased robustness while maintaining the same time duration as the ZVD shaper (one cycle of vibration). The only cost is the tolerance of some low-level residual vibration.

3.2 Sensitivity Curves

The vibration reduction characteristics of the input shapers are compared using the sensitivity curves in Fig. 3. As the ZV shaper is very sensitive to modeling errors, a small error in the modeling frequency leads to a significant residual vibration. On the other hand, the ZVD shaper has considerably more insensitivity to modeling errors, which is evident by noting that the width of the ZVD curve is much larger than the width of the ZV curve. The EI shaper has essentially the same length as the ZVD shaper, but it is considerably more insensitive.

To quantify the robustness of shapers, we define a performance measure for a shaper's sensitivity to modeling errors. Insensitivity I is the width of the sensitivity curve at a given level of vibration (tolerable vibration, V_{tol}). Vibration levels of 3% and 5% are commonly used to calculate insensitivity (I_3 and I_5 , respectively). Then, insensitivity I presents the effectiveness of the input shaper at a specific level of vibration.

3.3 Assumptions for Applying Input Shaping Control to Crane Systems

It requires the following assumptions to apply the input shaping control to crane systems.

(a) Initial conditions are all zeros.

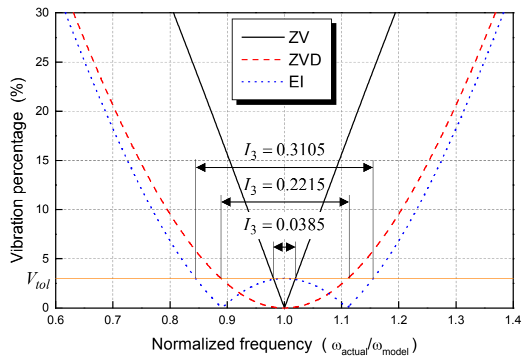

Fig. 3 Sensitivity curves of ZV, ZVD, and EI (V_{tol} =3%) shapers.

(b) The motor driver outputs the desired trolley acceleration and an ideal velocity control of the trolley is achieved.
(c) Only the sway dynamics are considered and the motor dynamics are excluded in generating the control input.
(d) There are no external disturbances: Even if external disturbances exist, those do not change the system dynamic characteristics.
(e) No feedback loop is present to account for the unmodeled dynamics: Only feedforward controller is applied to the crane system.
(f) The sway angle is small enough to lead to the linear approximation.

4. INPUT SHAPING WITH ANGLE CONSTRAINT

Solutions of (4)-(7) and V =0 will lead to commands that reduce residual vibration and ensure robustness to modeling errors. However, the sway of the payload suspended in the crane system during the traveling has not been considered. If the sway is large, the crane structure may be damaged, or an operator can be in danger in case of emergency.

4.1 Expression for the Sway Angle

To limit the magnitude of sway angle during the traveling, an expression for the sway angle as a function of the amplitudes and time locations of the input shaper must be found. The desired function can be obtained using superposition property of sway angle responses from individual step inputs.

An expression for the sway angle of the crane system is derived using the Laplace transform. The Laplace transform of the equation of motion for system (3) is

$$\left(s^2+\frac{g}{L}\right)\Theta(s)=\frac{1}{L}U(s), \tag{8}$$

where $U(s)=A/s$ (assuming $u(t)$ is a step input of magnitude A). Therefore, we have

$$\Theta(s)=\frac{A}{L\omega^2}\frac{\omega^2}{s(s^2+\omega^2)}, \tag{9}$$

where $\omega=\sqrt{g/L}$ is the natural frequency of system oscillation.

Taking the inverse Laplace transform of equation (9), assuming zero initial conditions, gives the sway angle from a step input with magnitude A as a function of time as follows:

$$\theta(t)=\frac{A}{L\omega^2}L^{-1}\left[\frac{\omega^2}{s(s^2+\omega^2)}\right]=\frac{A}{g}(1-\cos\omega t). \tag{10}$$

Multiple versions of (10) can be used to obtain a function that describes the transient sway angle throughout a traveling containing many step inputs. Assuming that the shaped command profile consists of a series of pulses obtained by convolving reference profile with input shaper, the sway angle throughout the traveling is given by

$$\theta(t)=\theta_{(k)\sim(k+1)}(t)=\sum_{j=1}^{k}\frac{A'_j}{g}\left(1-\cos\omega(t-t'_j)\right),$$

$$t'_k\le t\le t'_{k+1},\ k=1,\ldots,M \tag{11}$$

where the prime symbol exhibits the amplitude and time location of the shaped command profile, and M is the number of total steps in command profile as shown in Fig. 4. Therefore, each segment is described by

$$\theta_{1\sim2}(t)=\frac{A'_1}{g}\left(1-\cos\omega(t-t'_1)\right)=\frac{A'_1}{g}\left(1-\cos\omega t\right),\ 0\le t\le t'_2, \tag{12}$$

$$\theta_{2\sim3}(t)=\frac{A'_1}{g}\left(1-\cos\omega t\right)+\frac{A'_2}{g}\left(1-\cos\omega(t-t'_2)\right),\ t'_2\le t\le t'_3, \tag{13}$$

$$\vdots$$

$$\theta_{(M)\sim(M+1)}(t)=\frac{A'_1}{g}\left(1-\cos\omega t\right)+\frac{A'_2}{g}\left(1-\cos\omega(t-t'_2)\right)$$
$$+\cdots+\frac{A'_M}{g}\left(1-\cos\omega(t-t'_M)\right),\ t'_M\le t. \tag{14}$$

4.2 Limiting the Transient Sway Angle

One method to limit the maximum transient sway angle is to find all of the local extreme points of the sway angle function and limit the angle amplitude within a specified value at these instances. To obtain the extreme points of the sway angle, (11) is differentiated with respect to time and the result is set equal to zero. The time values satisfying the resulting equation correspond to the extreme points.

Differentiating (12) for the sway angle between t'_1 and t'_2, $\theta_{1\sim2}(t)$ and setting the result to zero, we obtain

$$\frac{d\theta_{1\sim2}}{dt}=\frac{A'_1\omega}{g}\sin\omega t=0. \tag{15}$$

(15) is satisfied by $t=i\pi/\omega$ ($i=1,3,\ldots$) when the magnitude of the sway angle is at a maximum. If we require that (12) be less than a desired value at $t=\pi/\omega$, then we have obtained a limited sway angle constraint equation that is a function of a specified time.

$$\theta_{1\sim2}\left(\frac{\pi}{\omega}\right)=\frac{A'_1}{g}\left(1-\cos(\pi)\right)=\frac{2A'_1}{g}\le\theta_{tol}, \tag{16}$$

where θ_{tol} is a tolerable sway angle. Also, the location of the extreme point between t'_k and t'_{k+1} is

$$t_{(k)\sim(k+1)}=\frac{1}{\omega}\tan^{-1}\left(\frac{A'_2\sin\omega t'_2+A'_3\sin\omega t'_3+\cdots+A'_k\sin\omega t'_k}{A'_1+A'_2\cos\omega t'_2+A'_3\cos\omega t'_3+A'_k\cos\omega t'_k}\right). \tag{17}$$

The extreme points given by (17) are substituted back into the appropriate segment of (11) and the resulting equations are constrained to be below the tolerable sway angle, θ_{tol}.

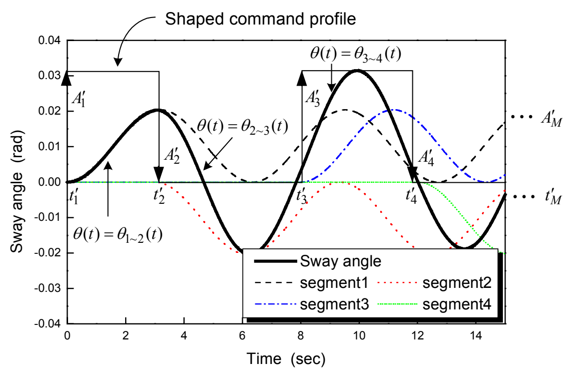

Fig. 4 Generation of the sway angle function during traveling.

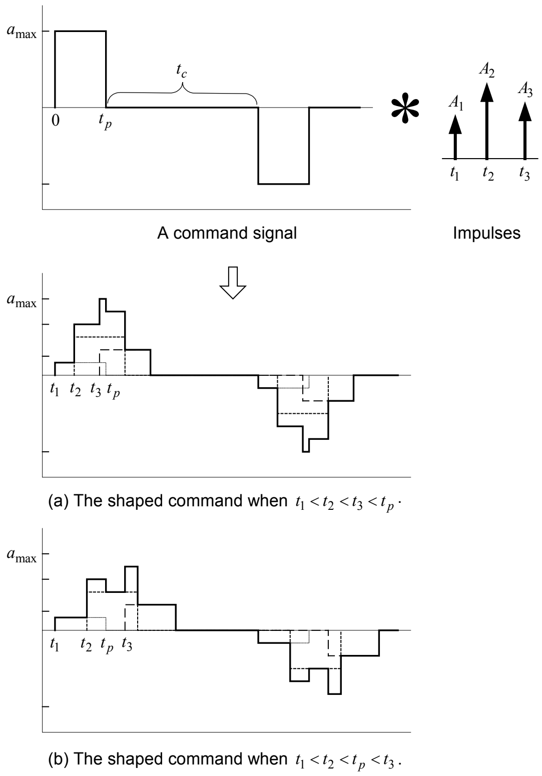

Fig. 5 The command shaping process for the bang/off-bang profile.

5. SHAPER DESIGN AND SIMULATIONS

In this section, various shapers together with the reference input, i.e. unshaped input, for the trolley to reach the traveling distance are first designed and then computer simulations are carried out with the parameters introduced in Section 2.3. If the oscillation of the payload is ignored, then time-optimal inputs can be easily calculated using the maximum acceleration, a_{max}, and the maximum velocity, v_{max}, of the system (Hong et al., 1997; Singhose et al., 2000). The maximum values of the acceleration and the velocity are the same as Table 1. For the bang/bang profile, the command switching time, t_s, is

$$t_s = \sqrt{\frac{x_d}{a_{max}}}, \tag{18}$$

where x_d is the traveling distance. The acceleration command is bang/off-bang when

$$x_d > v_{max}^2 / a_{max} . \tag{19}$$

In this case, the pulse duration, t_p, is

$$t_p = \frac{v_{max}}{a_{max}}, \tag{20}$$

and the coast period, t_c, is

$$t_c = \frac{x_d}{v_{max}} - \frac{v_{max}}{a_{max}} . \tag{21}$$

Now, if this unshaped time-optimal rigid-body input is convolved with the proposed input shapers, then the shaped input without exceeding the maximum velocity, v_{max}, as well as the maximum acceleration, a_{max}, of the system is generated as shown in Fig. 5. One thing to note is that the profile of the shaped command depends on the amplitudes and time locations of the shaper and the pulse duration, t_p, of the reference command signal. Suppose that the input shaper consists of three impulses and the sequence of pulse locations are $t_1 < t_2 < t_s < t_p$, then the amplitude, A_i', and time locations, t_i', of the modified input shaper are

$$\begin{bmatrix} A_i' \\ t_i' \end{bmatrix} = \begin{bmatrix} A_1 & A_2 & A_3 & -A_1 & -A_2 & -A_3 & \cdots \\ t_1 & t_2 & t_3 & t_p & t_p + t_2 & t_p + t_3 & \cdots \end{bmatrix}, \; i = 1, \cdots, 12 \tag{22}$$

as shown in Fig. 5(a). However, if $t_1 < t_2 < t_p < t_3$ is assumed, the shaped command becomes

$$\begin{bmatrix} A_i' \\ t_i' \end{bmatrix} = \begin{bmatrix} A_1 & A_2 & -A_1 & A_3 & -A_2 & -A_3 & \cdots \\ t_1 & t_2 & t_p & t_3 & t_p + t_2 & t_p + t_3 & \cdots \end{bmatrix}, \; i = 1, \cdots, 12 \tag{23}$$

as shown in Fig. 5(b).

5.1 Design of Shapers

As described in Section 3, the solution of (4)-(6) and V =0 will lead to the ZV input shaper that eliminates only residual vibration when the model is exact (L =15 m). The ZVD shaper, that has some level of robustness to modeling errors, is determined by adding one more constraint (7).

ZV shaper:

$$\begin{bmatrix} A_i \\ t_i \end{bmatrix} = \begin{bmatrix} 0.5 & 0.5 \\ 0 & 3.8847 \end{bmatrix}. \tag{24}$$

ZVD shaper:

$$\begin{bmatrix} A_i \\ t_i \end{bmatrix} = \begin{bmatrix} 0.25 & 0.5 & 0.25 \\ 0 & 3.8847 & 7.7695 \end{bmatrix}. \tag{25}$$

Modified input shapers are now obtained by solving (4)-(7) and an additional constraint limiting the sway angle, for example, within 0.0120 radian (about 0.7°). The amplitudes and time locations of the input shapers presented here are obtained by solving a set of constraint equations, (4)-(7), (11), and (17), using a nonlinear optimization program (Brooke et al., 1998).

ZV_C shaper:

$$\begin{bmatrix} A_i \\ t_i \end{bmatrix} = \begin{bmatrix} 0.2542 & 0.4915 & 0.2542 \\ 0 & 4.2048 & 8.4097 \end{bmatrix}. \tag{26}$$

ZVD_C shaper:

$$\begin{bmatrix} A_i \\ t_i \end{bmatrix} = \begin{bmatrix} 0.1257 & 0.3743 & 0.3743 & 0.1257 \\ 0 & 3.7755 & 7.5502 & 11.3258 \end{bmatrix}. \tag{27}$$

5.2 Simulation Results

A simple single-pendulum crane model with a single linear flexible mode is investigated. The system responses to the shaped input signals are compared in Fig. 6. When the model is exact as a LTI system, the shapers reduce the residual sway distance of the payload to zero exactly at the target point. However, as hoisting occurs, the shapers yield small residual vibration. The modified input shapers, which are in Table 2, are more effective than other conventional shapers in limited transient sway angle and 3% insensitivity range as shown in Fig. 6 and Fig. 7. The only penalty is that the traveling times of the proposed input shapers are increased as 11.6% and 8.3%, respectively.

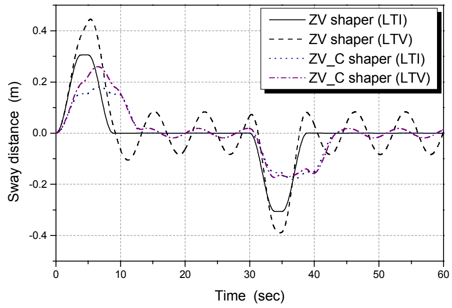

(a) Sway distance: ZV and ZV with an angle constraint (0.012 rad)

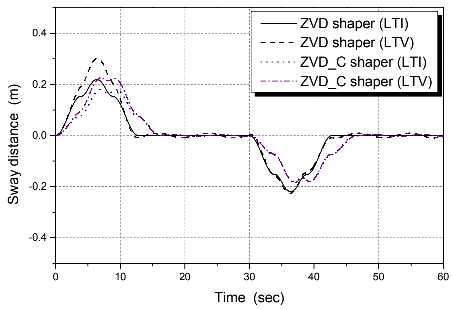

(b) Sway distance: ZVD and ZVD with an angle constraint (0.012 rad)

Fig. 6 Comparison of the time responses with shaped inputs.

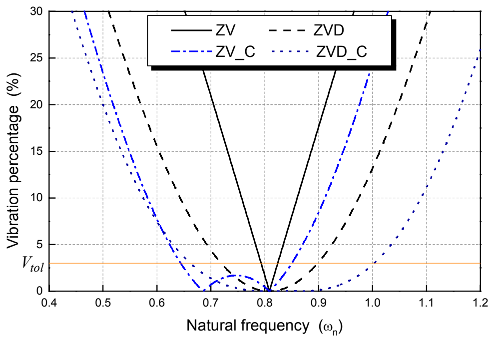

Fig. 7 Sensitivity curves: ZV, ZVD, ZV with an angle constraint, and ZVD with an angle constraint (θ_{tol} =0.012 rad).

6. CONCLUSTIONS

In this paper, a modified input shaping control design method to reduce residual vibration at the end-point and to limit the sway angle of the payload during traveling in crane systems was investigated. The reduction of both residual vibration and transient sway was demonstrated with computer simulations using crane model incorporating the change of rope length. The only penalty of the modified input shapers was that the traveling time of the crane system was increased. However, considering the safety in the presence of winds, the modified input shaping method was shown to be more effective than other conventional shapers in fulfilling three objectives: to limit the transient sway angle within a specified value, to achieve the minimal residual sway distance, and to provide robustness in rope length change.

ACKNOWLEDGMENT

This work was supported by the Brain Korea 21 Program of the Ministry of Education and Human Resources, Korea.

Table 2 Simulations of simple single-pendulum. (LTI: L =15 m and LTV: L =21 m→15 m)

Shapers	Model	Max. transient sway angle (rad)	Max. residual sway distance (m)	Traveling Time (sec)	Insensitivity I_3
ZV	LTI	0.0204	0	38.885	0.0310
	LTV	0.0260	0.0833		
ZV_C	LTI	0.012	0	43.410	0.2060
	LTV	0.0137	0.01817		
ZVD	LTI	0.01464	0	42.770	0.1790
	LTV	0.01505	0.0095		
ZVD_C	LTI	0.0120	0	46.326	0.3420
	LTV	0.0127	0.0041		

REFERENCES

Auernig, J. W. and Troger, H. (1987). Time Optimal Control of Overhead Cranes with Hoisting of the Load. *Automatica*, **23(4)**, 437-446.

Brooke, A., Kendrick, D., Meeraus, A., and Raman, R. (1998). *GAMS: A User's Guide*, GAMS Development Corporation.

Hong, K. S., Sohn, S. H., and Lee, M. H. (1997). Sway Control of a Container Crane (Part I): Modeling, Control Strategy, Error Feedback Control via Reference Velocity Profiles. *Journal of Control, Automation, and Systems Engineering*, **3(1)**, 23-31 (in Korean).

Hong, K. S., Park, B. J., and Lee, M. H. (2000). Two-Stage Control for Container Cranes. *JSME International Journal, Series C*, **43(2)**, 273-282.

Liu, Q. and Wie, B. (1992). Robust Time-Optimal Control of Uncertain Flexible Spacecraft. *Journal of Guidance, Control, and Dynamics*, **15(3)**, 597-604.

Meckl, P. H. and Seering, W. P. (1990). Experimental Evaluation of Shaped Inputs to Reduce Vibration for a Cartesian Robot. *ASME Journal of Dynamic Systems, Measurement, and Control*, **112**, 159-165.

Moustafa, K. A. F. and Ebeid, A. M. (1988). Nonlinear Modeling and Control of Overhead Crane Load Sway. *ASME Journal of Dynamic Systems, Measurement, and Control*, **110**, 266-271.

Park, B. J., Hong, K. S., and Huh, C. D. (2000). Time-Efficient Input Shaping Control of Container Crane Systems. *IEEE International Conference on Control Applications*, **MA4-6**, 80-85.

Park, J. and Chang, P. H. (1998). Learning Input Shaping Technique for Non-LTI Systems. *Proceedings of the 1998 American Control Conference*, 2652-2656.

Sakawa, Y. and Shindo, Y. (1982). Optimal Control of Container Cranes. *Automatica*, **18(3)**, 257-266.

Singer, N. C. and Seering, W. P. (1990). Preshaping Command Inputs to Reduce System Vibration. *ASME Journal of Dynamic Systems, Measurement, and Control*, **112**, 76-82.

Singhose, W., Seering, W., and Singer, N. (1994). Residual Vibration Reduction Using Vector Diagrams to Generate Shaped Inputs. *ASME Journal of Dynamic Systems, Measurement, and Control*, **116**, 654-659.

Singhose, W., Banerjee, A., and Seering, W. (1997). Slewing Flexible Spacecraft with Deflection-Limiting Input Shaping. *Journal of Guidance, Control, and Dynamics*, **20(2)**, 291-298.

Singhose, W., Porter, L., Kenison, M., and Kriikku, E. (2000). Effects of Hoisting on the Input Shaping Control of Gantry Cranes. *Control Engineering Practice*, **8(10)**, 1159-1165.

Smith, O. J. M. (1958). *Feedback Control Systems*, McGraw-Hill Company, Inc., New York, 331-345.